

Maspin Mediates Increased Tumor Cell Apoptosis upon Induction of the Mitochondrial Permeability Transition

Khatri Latha, Weiguo Zhang, Nathalie Cella, Heidi Y. Shi, and Ming Zhang*

Department of Molecular & Cellular Biology, Baylor College of Medicine, Houston, Texas

Received 14 April 2004/Returned for modification 18 June 2004/Accepted 7 December 2004

Maspin is a unique serpin with the ability to suppress certain types of malignant tumors. It is one of the few p53-targeted genes involved in tumor invasion and metastasis. With this in mind, we attempted to study the molecular mechanism behind this tumor suppression. Maspin-expressing mammary tumors are more susceptible to apoptosis in both implanted mammary tumors *in vivo*, a three-dimensional spheroid culture system, as well as in monolayer cell culture under lowered growth factors. Subcellular fractionation shows that a fraction of maspin (in both TM40D-Mp and mutant maspin Δ N cells) translocates to the mitochondria. This translocation of maspin to the mitochondria is linked to the opening of the permeability transition pore, which in turn causes the loss of transmembrane potential, thus initiating apoptotic degradation. This translocation is absent in the other mutant, maspin Δ RSL. It fails to cause any loss of membrane potential and also shows decreased caspase 3 levels, proving that translocation to the mitochondria is a key event for this increase in apoptosis by maspin. Suppression of maspin overexpression by RNA interference desensitizes cells to apoptosis. Our data indicate that maspin inhibits tumor progression through the mitochondrial apoptosis pathway. These findings will be useful for maspin-based therapeutic interventions against breast cancer.

Cancer cells are defective in their response to apoptosis. Unlike their normal counterparts, which undergo apoptosis in response to lower survival signals, tumor cells do not undergo apoptosis easily because they have defects in their ability to activate the death signaling pathway (17). Thus, one effective cancer therapy is to activate the tumor cell's apoptosis pathway (10, 11, 31).

Mammary serine protease inhibitor (maspin) was identified in normal mammary epithelial cells by subtractive hybridization as a candidate tumor suppressor protein. It is considered a class II tumor suppressor gene (43, 67) since the gene is not mutated or deleted but rather transcriptionally downregulated or silenced by epigenetic changes in breast cancer (14, 63, 68). A number of studies have shown its inhibitor effects on tumors. Mammary carcinoma cells transfected with maspin showed reduction in tumor growth and metastasis in nude mice (58). While the addition of recombinant maspin decreased the migration potential of breast and prostate cancer cells, the levels of maspin expression showed an inverse correlation with progression of malignancies (58). It has been documented that maspin inhibits angiogenesis in rat cornea and xenograft models (65) and has also been shown to inhibit mammary tumor progression and metastasis in bitransgenic mice (65).

In human breast tissue, maspin is expressed in both myoepithelial and luminal epithelial cells, and it has been suggested that the maspin-expressing myoepithelial cells form a defensive barrier to progression from ductal carcinoma *in situ* to more invasive carcinoma (49). Despite its proven role in tumor suppression, the molecular mechanism underlying maspin's inhibition is not well characterized. Previously, our laboratory

showed that mammary glands overexpressing maspin inhibited alveolar development during pregnancy through the induction of mammary cell apoptosis (64). Subsequently, we demonstrated that in mammary tumors from both whey acidic protein-simian virus 40 T antigen and whey acidic protein-maspin bitransgenic mice, there was a strong correlation between maspin overexpression and increased apoptosis (65), suggesting that maspin could directly induce tumor cell apoptosis *in vivo*. Jiang et al. (21) have also shown that maspin can sensitize MDA-435 mammary tumor cells to induce apoptosis by a chemical reagent.

There are at least two signaling pathways that are involved in apoptosis, the extrinsic and intrinsic pathways. The extrinsic pathway is activated by ligand-bound death receptors of the tumor necrosis factor receptor superfamily (6). The intrinsic pathway is a signal transduction pathway involving the mitochondria and the Bcl2 protein family (5). The role of mitochondria in the process of apoptosis has been the focus of attention ever since it was observed that the antiapoptotic protein Bcl2 localizes in the outer membrane of mitochondria (34). Over the past several years, permeabilization of the mitochondrial outer membrane to release proteins from the intermembrane space has been the focus of many researchers (59). Several of these, including cytochrome *c*, AIF, Smac/DIABLO, Omi/Htra2, and endoglycosidase G have all been found to have a role in the subsequent cell death (52, 8, 56, 27, 54). In particular, the release of cytochrome *c* induces the activation of caspase proteases through the induction of apoptosome formation (25).

Mitochondrial functions such as protein import, ATP generation, and lipid biogenesis depend on the maintenance of membrane potential ($\Delta\Psi_m$) (57), and loss of $\Delta\Psi_m$ during apoptosis likely causes cell death through these functions (37). Before cells manifest any signs of nuclear apoptosis, they disrupt the mitochondrial transmembrane potential (61). As to

* Corresponding author. Mailing address: Department of Molecular and Cellular Biology, Baylor College of Medicine, Houston, TX 77030. Phone: (713) 798-3817. Fax: (713) 798-3817. E-mail: mzhang@bcm.tmc.edu.

the mechanism of preapoptotic $\Delta\Psi_m$ disruption, it appears that it is mediated by so-called permeability transition pores, i.e., regulated megachannels that allow the dissipation of inner transmembrane ion gradients. There are known permeability transition inducers such as atractyloside, CaCl_2 , iodineamide, and also known chemicals which alternatively inhibit this $\Delta\Psi_m$ dissipation, such as cyclosporine and bongkrekic acid (62, 24).

A further argument in favor of the implication of permeability transition in apoptosis regulation is the finding that the apoptosis-inhibitory protein Bcl2 functions as an endogenous permeability transition inhibitor. This Bcl2 protective effect has been observed in both intact cells (61) and isolated mitochondria (62), suggesting that permeability transition may indeed constitute the Bcl2-regulated checkpoint(s) of the apoptotic cascade (51). Based on the finding of other investigators who used a cell-free system to study the induction of permeability transition in isolated mitochondria, it can be concluded that there is a direct molecular link between preapoptotic $\Delta\Psi_m$ disruption and apoptosis.

In this study, we report that maspin inhibits mammary tumor progression by actively mediating increased tumor cell apoptosis. A mitochondrial death signal pathway is induced which involves the localization of imported maspin to the mitochondria, the dissipation of $\Delta\Psi_m$, and release of cytochrome *c*. These data may provide major clues for understanding the role of maspin in apoptosis regulation.

MATERIALS AND METHODS

Cell line and cell culture. The TM40D mammary tumor cell line was established from a primary tumor that arose in the serially transplanted TM40D preneoplastic outgrowth line (22, 66). TM40D cells were grown in Dulbecco's modified Eagle's medium-medium F12 with 2% fetal bovine serum, epidermal growth factor, and insulin as described previously (22).

TM40D cells were infected with retrovirus vector for establishing stable cell lines as described by Shi et al. (46). Briefly, human maspin cDNA was cloned into pS2-GFP, a retroviral vector that was derived from the pS2 family of retroviral vectors. The plasmid constructs pS2-maspin and pS2-blank vector were transfected into 293T cells to produce infective viral particles. The viral supernatants were then allowed to infect TM40D cells in the presence of Polybrene. The transfected cells were then selected in the presence of 100 μg of zeocin (Invitrogen Co.) per ml. Cells were seeded by limiting dilution in 96-well plates. Single clones of stably transfected cells were transferred to individual wells of 24-well plates and cultured in medium containing 100 μg of zeocin per ml. Individual clones were confirmed for the presence of human maspin cDNA by reverse transcription-PCR, immunoblotting with maspin polyclonal antibody, and immunofluorescence staining.

Two maspin overexpression clones were chosen and named TM40D-Mp(16) and TM40D-Mp(18). One TM40D cell line infected by the pS2 vector was used as a negative control. All the subclones were subsequently maintained at 37°C in a humidified 95% O_2 -5% CO_2 atmosphere in Dulbecco's modified Eagle's medium supplemented with 10% fetal bovine serum and L-glutamine. For spheroid cell culture, the subclone cells were seeded in nonprecoated culture dishes and cultured in 37°C-5% CO_2 incubator with shaking for 3 days (53). As a result, cells did not attach to the substratum but simply grew and formed small three-dimensional colonies. They were then transferred to Matrigel-covered petri dishes and kept in culture for 1 week.

Conditions for apoptosis induction. TM40D and TM40D-MP cells were plated on coverslips or 10-cm plates and cultured to 80% confluence. They were serum starved for 48 h in Dulbecco's modified Eagle's medium with 1% penicillin-streptomycin. The DNA fragmentation assay was carried out by a modification of Stolzenberg's protocol (50). After serum starvation for 48 h, the cell lines were collected by centrifugation for 3 min at 1,200 rpm, washed with ice-cold phosphate-buffered saline buffer, and lysed in DNA extraction buffer (50 mM Tris-HCl [pH 8.0], 100 mM EDTA, 100 mM NaCl, 1% sodium dodecyl sulfate, and 0.3 mg of proteinase K per ml) for at least 3 h at 55°C. The DNA was precipitated by the addition of isopropanol with subsequent centrifugation at

14,000 rpm for 10 min and washed with 70% and 100% ice-cold ethanol. Following the removal of ethanol, the DNA was air dried and dissolved in 20 μl of Tris-EDTA buffer; 5 μg of DNA was analyzed on a 1.6% agarose gel and visualized under UV light.

Cells were also induced to apoptosis by the chemical reagent staurosporine; 1 μM staurosporine was added to Dulbecco's modified Eagle's medium with 2.5% fetal bovine serum for 4 h.

TUNEL assay. After serum starvation, the cells cultured on coverslips were washed with ice-cold phosphate-buffered saline and fixed in 4% paraformaldehyde for 1 h at 4°C. The TUNEL (terminal deoxynucleotidyl transferase-mediated dUTP nick end labeling) assay was performed according to the manufacturer's specifications (Roche). They were then rinsed with phosphate-buffered saline twice and permeabilized with 0.1% Triton X-100 in 0.1% sodium citrate for 2 min on ice. Following the Triton treatment, 50 μl of TUNEL reaction mixture was added to each sample for 30 min at 37°C. The slides were then rinsed three times with phosphate-buffered saline and counterstained with 4',6'-diamidino-2-phenylindole (DAPI). They were analyzed with fluorescence microscopy. The quantitation of apoptosis was done by counting the number of apoptotic cells in four randomly selected fields with a 20 \times objective. For the tumor section TUNEL assay, tumor samples were embedded and sectioned to 5- μm slides. The in situ TUNEL assay was carried out for sections as described above. The number of mammary cancer cells undergoing apoptosis was determined by counting the number of apoptotic cells per $\times 200$ field. Three such fields were counted for each tumor sample, and the numbers were averaged.

Sub-G₁ DNA content measured by flow cytometry analysis. TM40D cells in monolayers or spheroids were grown in the absence of serum as mentioned above for apoptosis analysis. Flow cytometry was used to measure the sub-G₁ DNA content, a marker for the fraction of apoptotic cells. Briefly, cells were first collected by trypsinization and fixed with 70% cold ethanol for 1 h at room temperature with shaking and then washed with phosphate-buffered saline twice and finally incubated with RNase and stained with propidium iodide for 30 min at 37°C. The DNA content was analyzed with Beckman-Coulter EPICS with a 15-mW argon laser at 488 nm and System II version 3.0 program.

Subcellular fractionation. Subcellular fractionation of TM40D-Mp cells was performed as described previously (16). Each fraction was subjected to two cycles of washing to remove cross contamination and further analyzed for maspin content by sodium dodecyl sulfate (SDS)-polyacrylamide gel electrophoresis (PAGE). The purity of each fraction was also tested by immunoblotting with various fraction markers.

Construction, expression, and purification of His/GST-maspin fusion proteins. Glutathione S-transferase (GST)-maspin containing a C-terminal deletion (maspin Δ RSL) has been described previously (65). Deletion of amino acids 140 to 375 (N-maspin) and 1 to 139 (maspin Δ N) was constructed in the same way as outlined in reference 65. They were transformed into *Escherichia coli* BL21 cells and expressed and purified as described by the manufacturer (Amersham Pharmacia Biotech). Similarly, the His-maspin fusion protein was already available from the laboratory stock, and they were expressed and purified according to the manufacturer's (BD Biosciences Clontech) instructions. The fusion proteins were then labeled with iodine-125 according to the manufacturer's protocol (Pierce) with Iodo-gen precoated iodination tubes. These were used for the import assay studies.

Plasmids, cell culture, and transfections. Constructs expressing the GST fusion proteins N-maspin, maspin Δ N, and maspin Δ RSL were generated by PCR-based cloning. Briefly, DNA fragments encoding the desired maspin regions in all the above constructs were produced by PCR amplification, digested with either EcoRI or XhoI and XbaI, and cloned into a pEF-IRES-P vector (18) digested with the same pair of enzymes. TM40D cells were maintained in Dulbecco's modified Eagle's medium supplemented with 5% fetal bovine serum. For the stable transfections, cells were plated in a 100-mm plate, and after about 70% confluency, the cells were transfected with the above plasmids by the use of Lipofectamine (Life Technologies) according to the manufacturer's protocol. After transfection the cells were incubated in Dulbecco's modified Eagle's medium-10% fetal bovine serum for 48 h, and selection with puromycin (1 $\mu\text{g}/\text{ml}$) was started. The cells under selection were grown for about 2 to 4 weeks for stable transfections and then harvested and further analyzed.

Isolation of mitochondria and import of maspin. Mitochondria from mouse liver were prepared according to the protocol outlined by Susin et al. (52). The import assay was done according to Ryan et al. (42). For protease treatment, the samples were cooled to 0°C and incubated with proteinase K (30 $\mu\text{g}/\text{ml}$) for 20 min at 0°C. Then a 30-fold excess of phenylmethylsulfonyl fluoride was added to the samples. The mitochondria were then reisolated by centrifugation and analyzed by SDS-PAGE, and phosphorimage analysis for the ¹²⁵I-labeled maspin and ovalbumin and also for the other GST fusion proteins. Atractyloside (5 mM)

was added to see whether opening of the permeability transition pore facilitated import (52). Mitochondria from cells were isolated according to the protocol of Yang et al. (60). The isolated mitochondria were then analyzed by SDS-PAGE and checked for the expression of maspin by Western blotting and Immunoprecipitation analysis.

Membrane integration and fractionation. Mitochondrial swelling was performed according to Sollner et al. (47). After import, mitochondria were diluted with five times their volume of SEM buffer or EM buffer (the same buffer without sucrose in order to induce hypo-osmotic shock of the mitochondria) in the presence of proteinase K (30 $\mu\text{g/ml}$) for 20 min at 0°C. Phenylmethylsulfonyl fluoride was added, and the mitochondria were pelleted, rinsed, and resuspended in sample buffer. Carbonate extraction was done by the procedure outlined by Ryan et al. (42). Submitochondrial fractions (matrix, inner membrane, intermembrane space, and outer membrane) were obtained following standard methods (36).

Membrane potential ($\Delta\Psi\text{m}$) dissipation. The staining protocol for fluorescence ratio detection was done per the protocol outlined in the manufacturer's catalogue (Biocarta). The cells were prepared and stained with JC-1 dye as per the method outlined by Biocarta and analyzed with a fluorescence plate reader.

Fluorescence plate reader set-up. The plate reader was set up to perform an endpoint read. The excitation wavelength was set at 488 to 490 nm, and the emission wavelength was set at 527 nm for green fluorescence and at 590 to 600 nm for red fluorescence. The samples were read under these set conditions.

Release of cytochrome *c*. Cytochrome *c* release from TM40D and TM40D-Mp cells and cytochrome *c* immunoblotting were carried out with a modified protocol of Kluck et al. (23). Cultured cells were starved with serum-free Dulbecco's modified Eagle's medium for 48 h and then collected with lysis buffer (50 mM Tris [pH 7.5], 150 mM NaCl, 5 mM EGTA, 1 mM CaCl₂, 1 mM MgCl₂, 1% NP-40, 1 μg of leupeptin per ml, 1 μg of aprotinin per ml, 1 μM phenylmethylsulfonyl fluoride, and 100 μM Na₃VO₄) and left incubating at 4°C either for 2 h or overnight. After the lysis they were centrifuged at 14,000 rpm for 15 min. The supernatants were collected, and total cytosolic proteins were quantitated by Bradford spectrometer. About 100 μg of protein was loaded in an SDS-12.5% PAGE gel and transferred to a polyvinylidene difluoride membrane (Bio-Rad Laboratories, Richmond, Calif.) at a constant current of 250 mA for 2 h.

Western blotting and immunoprecipitation. For Western blotting analysis, cell lysates were prepared with a low-salt buffer as described unless otherwise specified. They were separated by SDS-PAGE followed by Western blotting on nitrocellulose membranes and immunodetection of cytochrome *c* (H-104, Santa Cruz; dilution 1:1,000) and OGC (dilution 1:500). Then, membranes were incubated with anti-rabbit immunoglobulin G-horseradish peroxidase conjugate (dilution 1:1,000). Antibody-conjugated activity was visualized with the Super Signal chemiluminescence reagent (Pierce). For immunoprecipitation analysis, whole-cell lysates and/or the cytoplasmic and mitochondrial fractions were incubated overnight with the maspin antibody. Immune complexes were precipitated with protein A-Sepharose beads and washed with lysis buffer before being resolved on SDS-PAGE and analyzed by Western blotting.

RNA interference. Sequences of silencing short interfering RNAs in the maspin mRNA were selected based on a previously described method (9). In order to identify effective knockdown short interfering RNAs, we initially selected two potential target sequences in maspin mRNA and synthesized short interfering RNA duplexes (silencer short interfering RNA construction kit; Ambion). A commercially available negative-control short interfering RNA was used as a control (sequence 1; Ambion). Short interfering RNA sequences were transiently transfected into cells with Oligofectamine (Invitrogen), and maspin expression was analyzed by Western blotting. Effective and specific short interfering RNAs were cloned into the pSUPER.retro.puro vector (Oligo Engine) and transfected into the PT67 packing cell line (Clontech). Virus-containing supernatants were added to TM40D-Mp cells for 2 days in the presence of 2 μg of Polybrene. An empty pSUPER.retro was used as a control. Two days after infection, cells were treated with 1 μg of puromycin for 2 to 4 days. Cells stably expressing maspin short interfering RNAs were used for further analysis.

Caspase-3 fluorogenic assay. Cells were seeded in triplicate in a 96-well plate and grown to about 80% confluence either with or without inducers for apoptosis. The growth medium was aspirated and 30 μl of lysis buffer (1 \times lysis buffer: 10 mM Tris-HCl [pH 7.5], 10 mM NaH₂PO₄ or Na₂HPO₄ [pH 7.5], 130 mM NaCl, 1% Triton X-100, and 10 mM sodium pyrophosphate, sterile filtered and stored at 4°C) was added and incubated on ice for 30 min. During the incubation time, reaction mixtures were made up (for one well: 3.57 μl of Ac-DEVD-AMC caspase 3 fluorogenic substrate [Pharmingen catalog no. 66081U] reconstituted in 1 ml of dimethyl sulfoxide to yield a 1.4 mM final solution) and 216 μl of 1 \times protease assay buffer (20 mM HEPES [pH 7.5], 10% glycerol, 2 mM dithiothreitol added before use at 2 μl of 1 M dithiothreitol per ml of base). About 220 μl

of reaction mixture was added to each well (250 μl final volume), wrapped in aluminum foil, and incubated at 37°C for 3 to 6 h. The AMC liberated was measured with a fluorometer (excitation wavelength 360 nm and emission wavelength 465 nm).

RESULTS

Maspin mediates increased induction of mammary tumor apoptosis. To determine whether maspin overexpression has an effect on tumor progression *in vivo*, we carried out tumor implantation studies with the TM40D cell line. Two groups of mice were implanted with either maspin overexpression transfectants or control transfectants in both number 4 mammary glands. Since overexpression significantly inhibited mammary tumor growth and metastasis, we went on to determine whether this overexpression has any effect on tumor apoptosis. Primary tumors from TM40D and TM40D-maspin (TM40D-Mp) cells were sectioned, and *in situ* detection of apoptosis was performed (Fig. 1A and B). Increased apoptosis (about 40 to 50%) was seen in tumors expressing maspin compared to those without maspin (Fig. 1C).

In order to investigate the molecular mechanism underlying maspin-induced tumor cell apoptosis *in vivo*, stable clones with various levels of maspin expression were selected and analyzed by semiquantitative reverse transcription-PCR (data not shown). Two maspin-overexpressing clones TM40D-Mp(16) and TM40D-Mp(18), and a negative control subclone named TM40D(control) were selected for further study. TM40D-Mp(18) had higher maspin expression than TM40D-Mp(16) at both the mRNA and protein levels.

Multicellular spheroids are an excellent culture system for mimicking tumor growth *in vivo* (44). TM40D(control) and maspin-expressing TM40D-Mp cells were cultured to form three-dimensional spheroids in medium containing 10% serum (Fig. 2A to D). These spheroids were harvested, embedded in paraffin, and sectioned to 5- μm slides for hematoxylin and eosin staining histology and for the TUNEL apoptosis assay. The TUNEL assay revealed that TM40D-Mp(18) tumor cells had a higher rate of apoptosis than TM40D(control) cells (Fig. 2E and F). To further quantitate the difference of apoptosis between maspin-expressing TM40D-Mp tumors and TM40D control tumors, spheroids were harvested to measure apoptosis by a semiquantitative flow cytometry analysis. As shown in Fig. 2G, the sub-G₁ DNA content was measured as a fraction of apoptosis in the three TM40D cell lines. TM40D-Mp(16) and TM40D-Mp(18) cells had increased apoptosis compared to TM40D(control) cells (Fig. 2G).

To further confirm that maspin could increase tumor cell apoptosis under growth-limiting factors, TM40D and TM40D-Mp cells were grown in cell culture in the absence of serum for a fixed period of time, and the DNA fragmentation assay, a classical measurement for cell apoptosis, was carried out to measure the release of DNA fragments. An increase in DNA fragmentation was clearly observed in maspin-expressing (16) and TM40D-Mp(18) cells compared to TM40D cells (Fig. 3A). Furthermore, the TUNEL assay was used to quantitate the apoptosis level in the three TM40D tumor samples. When these tumor cells were grown under serum-free conditions for 24 h, apoptosis was induced in all three tumor samples. However, a significant increase in apoptosis was observed in

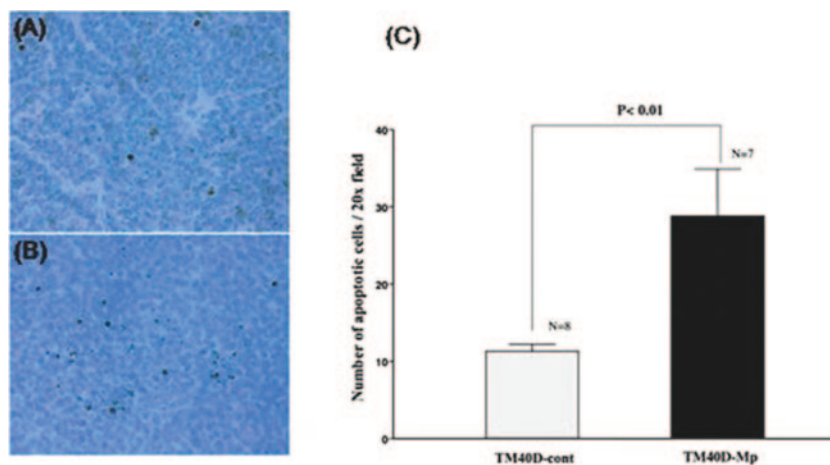


FIG. 1. In situ detection of apoptosis in mammary gland tumors by TUNEL analysis. (A and B) Representative apoptotic staining by TUNEL assay for (A) TM40D(control) and (B) TM40D-Mp maspin-expressing cells. (C) Summary of TUNEL analysis for both TM40D(control) and TM40D-Mp tumors. Bars represent standard errors. A significant difference was observed in tumor apoptosis between TM40D and TM40D-Mp samples.

TM40D-Mp cells compared to TM40D cells under serum starvation conditions (Fig. 3B). Moreover, under induced conditions (serum starved for 48 h), TM40D-Mp(18) cells were seen to have higher levels of maspin than TM40D-Mp(16). Hence, TM40D-Mp(18) cells were chosen for further study.

Localization of maspin in mitochondria. Subcellular fractionation (Fig. 4) of the cell extracts clearly indicates the ubiquitous distribution of maspin. While it is confined mostly to the cytosol (S4) in healthy TM40D-Mp cells with variable amounts in the nuclear (lanes P1), Golgi/lysosomal (lanes P3), and endoplasmic reticulum/microsomal fraction (lanes P4). After induction of apoptosis by serum starvation for 48 h, maspin translocates to the mitochondria (lanes P2 to 2) at the same time as a decrease in level in the cytosol (lanes S4 to 2) and a

slight increase in level in the endoplasmic reticulum (lanes P4 to 2). The level of maspin however remains the same in both the nuclear and Golgi/lysosomal fractions. With different marker antibodies against the different fractions, the purity of the fractionation was confirmed. Having found that the membranes are pure without any significant contamination of fractions, we strongly believe that maspin is translocated to the mitochondria under induced apoptotic conditions compared to healthy cells. This intrigued us to study the molecular mechanism behind the translocation of maspin into mitochondria.

Assaying protein import into mitochondria. The subcellular fractionation results revealed that maspin was translocated to the mitochondria when induced for apoptosis. Since mitochondrial translocation can be studied in vitro with the radioactively

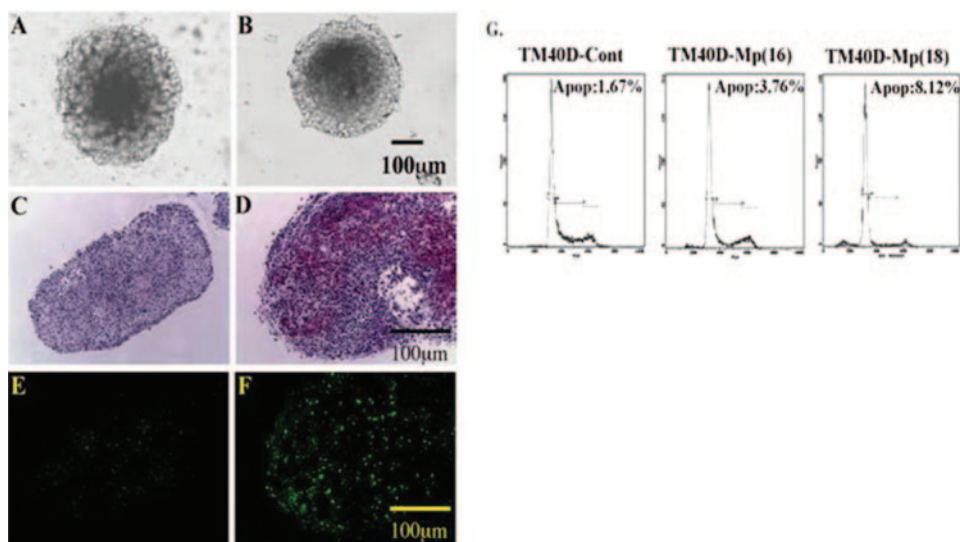


FIG. 2. Increased apoptosis in TM40D-Mp tumor spheroids assayed by TUNEL and flow cytometry. (A and B) Photographs of the three-dimensional structures of TM40D-control and TM40D-Mp(18) cells in culture by phase contrast microscopy. (C and D) Histology of tumor spheroids. (E and F) TUNEL staining of apoptotic cells in TM40D-control (E) and TM40D-Mp(18) (F) spheroids. (G) Flow cytometry analysis of apoptosis with tumor spheroids harvested from TM40D(control) and TM40D-Mp cells. Bars, 100 μ m.

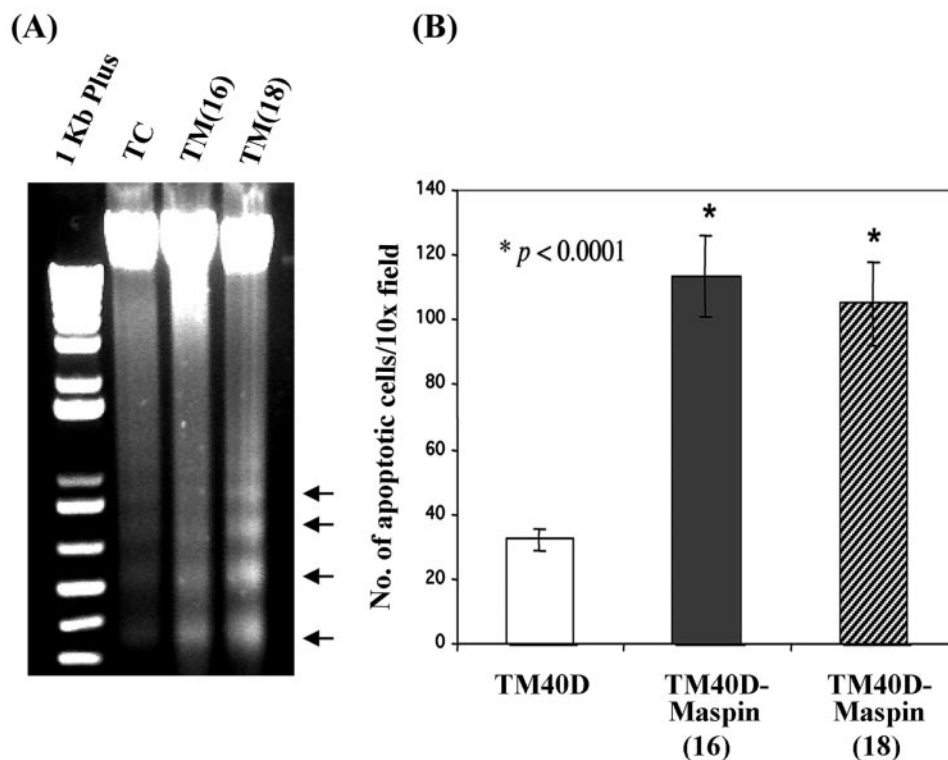


FIG. 3. Detection of increased apoptosis in TM40D-Mp cells in monolayer culture under serum starvation. (A) DNA fragmentation assay. After 48 h of serum starvation, total DNAs were extracted, and the same amount of DNA (5 μ g) was loaded in a 1.6% agarose gel for electrophoresis and visualized by ethidium bromide under UV. Arrows indicate DNA fragments. (B) TUNEL assay after 24 h of serum starvation. Apoptotic cells were counted in four randomly selected fields under a 10 \times objective. Results were from three independent experiments.

labeled protein of interest, we chose His-maspin (42 kDa) and labeled it with 125 I for the in vitro mitochondria import assay. Maspin was incubated with isolated mouse liver mitochondria to test its ability to interact with this organelle in vitro. The mitochondria were incubated in cell-free system buffer with or without atractyloside (5 mM) and then treated with proteinase K and reisolated by centrifugation. This was washed once with the cell-free system buffer and then centrifuged again. The pellet obtained is the mitochondrial fraction, and the supernatant is the cytosolic fraction.

As shown in Fig. 5A, maspin was found in the mitochondrial pellet in the presence of atractyloside (lane 1) but not in the absence of atractyloside (lane 2). Accordingly, maspin is found

in the supernatant in the absence of atractyloside (Fig. 5A, lane 4). Since most of the imported maspin in the presence of atractyloside is localized in the mitochondrial pellet, the supernatant fraction (Fig. 5A, lane 3) has little maspin present. To confirm the specificity of maspin import into mitochondria, ovalbumin (45 kDa), a member of the serpin family, which is also similar in size to maspin (42 kDa), was used as a control. Importantly, 125 I-labeled ovalbumin (Fig. 5B, lane 1) was not imported into the mitochondria even with the atractyloside incubation. Most of the labeled His-maspin under the noninduced conditions was found in the wash (since those protein molecules which were loosely bound to the mitochondria appeared to be removed in the wash) (data not shown), rational-

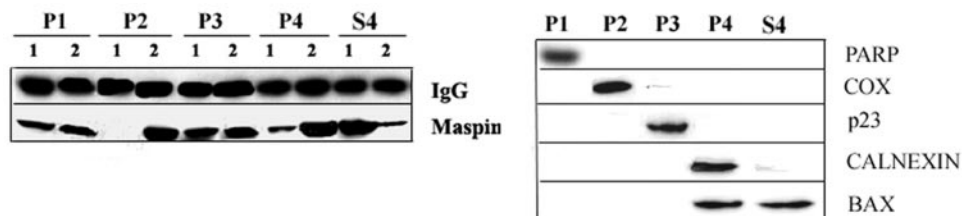


FIG. 4. Localization of maspin. Subcellular fractions were prepared from TM40D-Mp cells under noninduced (lane 1) and induced (lane 2) conditions as described in Materials and Methods and analyzed by immunoprecipitation and Western blotting for maspin. P1, pellet enriched in nuclear protein; P2, pellet enriched in mitochondrial proteins; P3, pellet enriched in lysosomal (Golgi) fraction; P4, pellet enriched in endoplasmic reticulum/microsomal fraction; S4, soluble cytosolic fraction. The fractions were tested for purity against procyelic acidic repetitive protein (PARP, a nuclear marker), COX (mitochondria), p23 (Golgi), calnexin (endoplasmic reticulum), and Bax (cytosolic fraction).

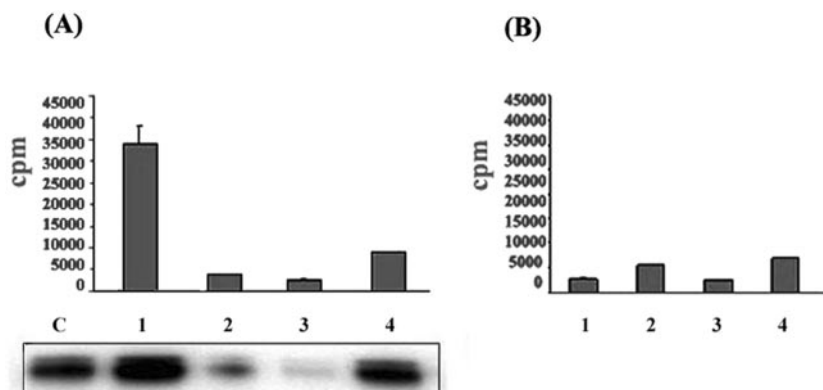


FIG. 5. In vitro import of maspin. Purified His-maspin was labeled with ^{125}I and the import assay was carried out as described in Materials and Methods. The results were analyzed by SDS-PAGE and by phosphorimage analysis. (A) Import of maspin. (B) Import of ovalbumin. (C) Phosphorimage analysis of maspin import under induced (addition of atractyloside) (lanes 1 and 3) and noninduced (lanes 2 and 4) conditions. Mitochondrial pellet fraction (lanes 1 and 2), supernatant (cytosolic) fraction (lane 3 and 4), and control ^{125}I -labeled His-maspin (lane C) are shown. The samples were counted in a Gamma counter, and bars show errors from three independent experiments.

izing the low level of labeled counts in the original supernatant fraction (Fig. 5A, lane 4, bar). This condition was also observed in ovalbumin under both induced and noninduced conditions (Fig. 5B, lanes 3 and 4) since the import of ovalbumin is not specific to mitochondria, the loosely bound proteins are washed away.

Determination of sublocalization of maspin in the mitochondria. To narrow down the localization of maspin more precisely, further experiments were carried out as outlined by Ryan et al. (42). We used the classical procedure for disruption of mitochondrial outer membrane by swelling the mitochondria. By swelling the matrix, imported maspin is seen to be protected from proteinase K (Fig. 6A, lanes 1 and 2). Therefore, it is either present free in the mitochondrial matrix or associated with the inner membrane. In addition, treatment with Triton X-100 before proteinase K digestion made it susceptible to protease degradation (Fig. 6A, lane 3). These results suggest that maspin is an integral mitochondrial protein.

Submitochondrial fractionation with the sodium carbonate extraction method indicated that maspin is present in the pellet fraction. Hence, it is resistant to alkaline extraction, suggesting that it is a transmembrane protein (Fig. 6A, lane 5), since proteins that remain in the pellet following extraction are hypothesized to be integral membrane proteins and proteins that remain in the supernatant are matrix proteins. This confirms that maspin is translocated to the inner membrane of mitochondria. Importantly, maspin was found in the same fractions as the oxoglutarate carrier OGC, an inner membrane marker protein (Fig. 6B, lanes 1 to 6). In order to confirm the localization of maspin in this inner membrane fraction, we carried out fractionation of the mitochondrial membrane. Imported maspin was found to be localized in the inner membrane fraction of the mitochondria (Fig. 7A and B, lane 4). Figure 7C (lane 4) depicts the expression of OGC in the inner membrane fraction obtained by fractionation.

To rule out the possibility of nonspecific interaction of the N-terminal His tag with mitochondrial membrane proteins, the import assay with GST-maspin was also done along with GST protein as a control (Fig. 8A and B). GST-maspin is found in the mitochondrial pellet and not in the supernatant in the

presence of atractyloside (lanes 1 and 3, respectively). However, in the absence of atractyloside, GST-maspin is found in the supernatant and not in the mitochondrial pellet fraction (lanes 4 and 2, respectively). To provide further support for the mitochondrial targeting of maspin, different mutant proteins of GST-maspin were studied for domain specificity for import into mitochondria. The mutant with only the N terminus of maspin did not get translocated into the mitochondria (Fig. 8C), whereas the mutant with the N-terminal deletion (maspin ΔN) (Fig. 8D) showed translocation. Furthermore, a deletion of 35 amino acids in the C terminus of maspin

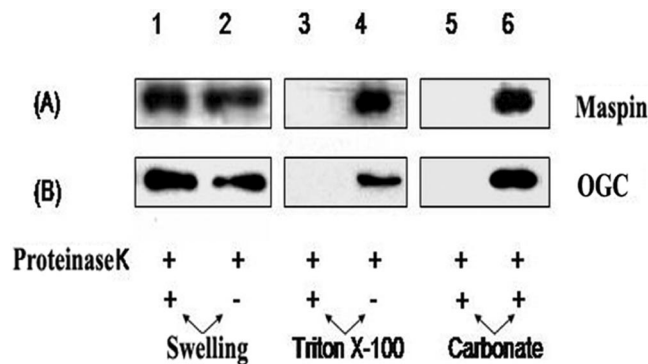


FIG. 6. Localization of imported maspin into mitochondria. To determine maspin sublocalization in mitochondria, the outer membrane was disrupted by either swelling, Triton extraction, or carbonate extraction (as described in Materials and Methods). (A) Immunoblot of maspin. Lanes 1 and 2, swelling. The remaining amount of maspin protected after proteinase K treatment were determined after formation of the mitoplast. Mitoplasts were obtained with an osmotic shock of 15 min in 1 mM EDTA–10 mM morpholinepropanesulfonic acid (MOPS, pH 7.2). Lanes 3 and 4, mitoplasts were treated with Triton X-100 or not before digestion with proteinase K, making them susceptible to proteinase K degradation. Lanes 5 and 6, carbonate extraction. The carbonate-resistant (pellet, lane 6) is separated from the peripheral carbonate-extractable proteins (supernatant, lane 5). (B) Immunoblot of OGC (a marker for the inner membrane protein) was also carried out in a similar way to follow the degree of opening of the mitochondrial outer membrane. This allowed observation of the specific localization of maspin to the inner membrane.

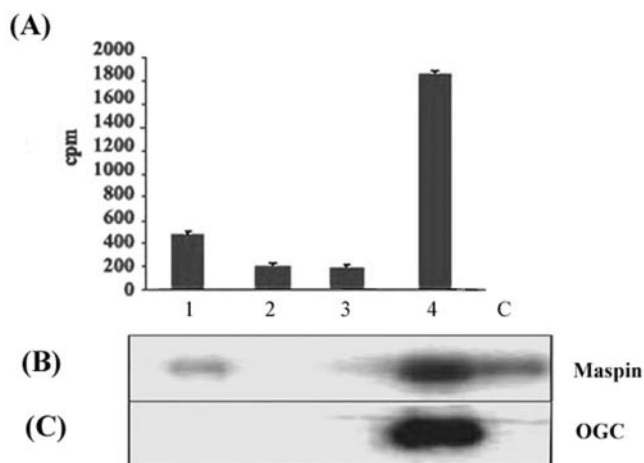


FIG. 7. Mitochondrial subfractionation. Isolated mitochondria were subfractionated according to standard protocols and analyzed by SDS-PAGE and phosphorimage analysis. Lanes: 1, matrix fraction; 2, outer membrane fraction; 3, intermembrane space; 4, inner membrane fraction. (A) The samples were counted in a Gamma counter, and the bar is representative of three experiments. (B) ^{125}I -labeled maspin was used as a control (lane c) and the imported ^{125}I -labeled maspin was visualized by phosphorimaging. (C) Immunoblot for OGC was also done to control fractionation.

(maspin Δ RSL), which contains the RSL domain, completely abolishes the ability of maspin to import to mitochondria and to induce apoptosis (Fig. 8E). The pattern of nonmitochondrial translocation with the other mutants, especially the one with the RSL domain deleted, highlights the fact that it is the RSL domain that appears to be important for the translocation of maspin into the mitochondria.

To further ascertain the role of mitochondrial import of maspin in apoptosis, these GST fusion constructs were PCR cloned into a mammalian expression vector and stably transfected to TM40D cells. After stable selection, the cells were harvested and fractionated to observe the localization of maspin in these mutants. It is clear from Fig. 9A that maspin is seen in the mitochondrial fraction only (lane P2) in the maspin Δ N transfectant clones but not in the maspin Δ RSL clones, clearly confirming the previous data with these mutants. It is also interesting that the subcellular fractionation of maspin Δ N is comparable to that of TM40D-Mp (Fig. 4, lane P2). These data clearly suggest that the translocation of maspin to the mitochondria is important for increased apoptosis in these cells.

To investigate further whether maspin indeed mediates increased apoptosis in the TM40D-Mp and various mutant transfectants, the caspase 3 assay was performed on these cells. The results (Fig. 9B) revealed that maspin Δ RSL and N-maspin transfectant clones did not induce effective apoptosis such as the TM40D-Mp cells did. However, there was a significant increase in the caspase 3 level of maspin Δ N transfectants when serum starved, and the caspase 3 activity level was comparable to that of TM40D-Mp cells. These data are consistent with the in vitro mitochondrial translocation assays (Fig. 8), suggesting that the ability of maspin to translocate to mitochondria is connected with the increased apoptosis and such an increase in apoptosis is mediated through the RSL domain of maspin.

Dissipation of membrane potential ($\Delta\Psi_m$). Detection of the mitochondrion permeability transition event provides an early indication of the initiation of cellular apoptosis. This is typically defined as a collapse in the electrochemical gradient across the mitochondrial membrane, as measured by a change in the membrane potential. We studied mitochondrial membrane collapse by the use of a fluorescent membrane potential probe, JC-1 (40), since atractyloside induction is known to open up the permeability transition pore. To study the dissipation of membrane potential in vivo, we proceeded to obtain the fluorescence ratio. With the dual fluorescence characteristic of the dye, the changes in the mitochondrial $\Delta\Psi_m$ can be most accurately assessed by comparing the ratio of optical density at 590 and 600 nm (red) with that at 527 nm (green). When apoptosis is induced, the red/green optical density ratio drops compared to that of the negative (noninduced) control. This drop in optical density corresponds to a reduction in the number of healthy mitochondria able to maintain the negative potential necessary to concentrate the dye in the red aggregate form. TM40D and TM40D-Mp cells were either induced for apoptosis by serum starvation or left noninduced and then labeled with the 1X JC-1 dye solution for 15 min. The samples were then read on a 96-well fluorescence plate reader with the settings described in Materials and Methods.

As the mitochondrial $\Delta\Psi_m$ collapses, indicating apoptosis, control cells had a 10% drop in red fluorescence (Fig. 10, TM40D, lane b) compared to the 75 to 80% red fluorescence drop in TM40D-Mp cells (Fig. 10, TM40D-MP, lane b). The

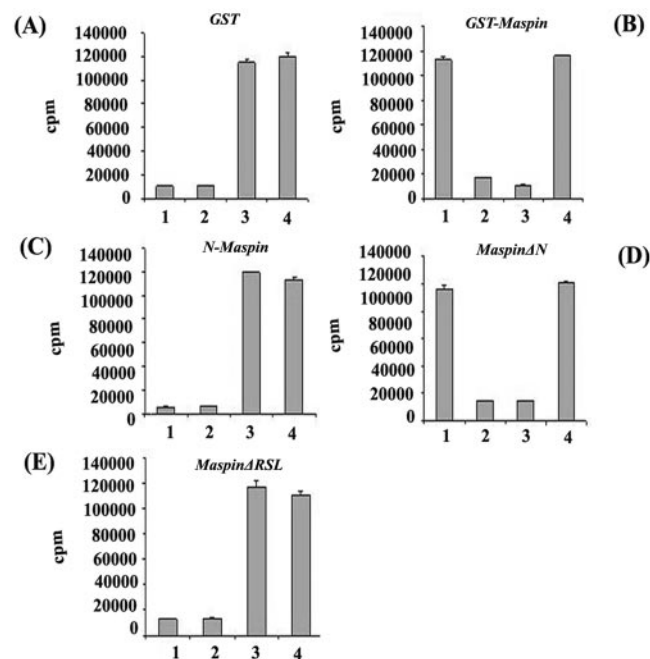


FIG. 8. Import of GST-maspin and other GST-maspin mutants. The import assay was performed under both induced (induced by atractyloside) (lanes 1 and 3) and noninduced conditions (lanes 2 and 4). Import assays were done with (A) GST (control); (B) GST-maspin; (C) N-maspin (GST-maspin with the N terminus alone); D, maspin Δ N (GST-maspin with the N terminus deleted); E, maspin Δ RSL (GST-maspin with the RSL domain deleted). Lanes: 1 and 2, mitochondrial pellet fraction; 3 and 4, supernatant (cytosolic) fraction.

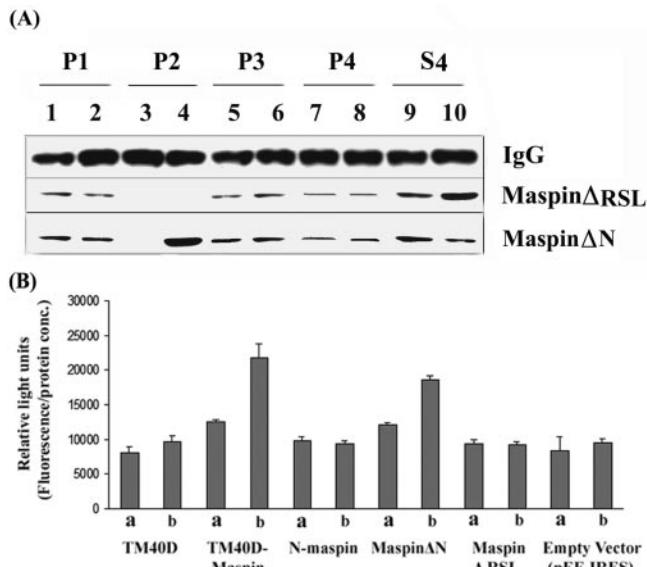


FIG. 9. (A) Subcellular fractions were prepared from maspin Δ N and maspin Δ RSL transfectant cells under noninduced (lane 1) and induced (lane 2) conditions as described in Materials and Methods and analyzed by immunoprecipitation and Western blotting for maspin. P1, pellet enriched in nuclear protein; P2, pellet enriched in mitochondrial proteins; P3, pellet enriched in lysosomal (Golgi) fraction; P4, pellet enriched in endoplasmic reticulum/microsomal fraction; S4, soluble cytosolic fraction. (B) Maspin plays a vital role in induced mitochondrial apoptosis. Caspase 3 fluorogenic assay of the control (TM40D and TM40D-Mp) cells and transfected TM40D cells with the DNA from constructs N-maspin, maspin Δ N, and maspin Δ RSL along with the empty vector (pEF-IRES-P) under noninduced (lanes a) and induced (48 h of serum starvation) conditions (lanes b).

transfectant clones maspin Δ N and maspin Δ RSL were also analyzed for this loss of $\Delta\Psi_m$. The maspin Δ N cells showed a drop of about 75% (Fig. 10, maspin Δ N, lane b), which is very close to that of TM40D-Mp cells, while maspin Δ RSL showed a drop of 10% (Fig. 10, maspin Δ RSL), which is comparable to that of the TM40D control cells. The increased loss of $\Delta\Psi_m$ in the TM40D-Mp and maspin Δ N cells is directly linked to the increased apoptosis activities in these cells, suggesting that the translocation of maspin into the mitochondria under induced membrane permeability transition triggers increased apoptosis in these cells.

Release of cytochrome *c* from mitochondria along with translocation of maspin into the mitochondria. Mitochondrial cytochrome *c* release appears to be a common change once the $\Delta\Psi_m$ is dissipated. Since maspin increases the loss of $\Delta\Psi_m$, we proceeded to study the release of cytochrome *c* in these maspin-overexpressing cells. For this purpose we analyzed cytochrome *c* release in TM40D and TM40D-Mp cells. Cells were serum starved and harvested for whole-cell extracts and mitochondrial and cytosolic fractions and subjected to Western blotting analysis for cytochrome *c* expression. As shown in Fig. 11A, the overall amount of cytochrome *c* in whole-cell extracts of TM40D and TM40D-Mp cells remained at the same level (whole-cell lysate panel). In the control TM40D cells, cytochrome *c* was found to be retained in the mitochondrial fraction even under induced conditions (lane 2, mitochondrial fraction) when compared to the noninduced conditions (Fig.

11A, lane 1, mitochondrial fraction). There is a low level of cytochrome *c* expression observed in the cytoplasmic fraction under induced conditions (Fig. 11A, lane 2, cytosolic fraction), indicating the low level of mitochondrial apoptosis in these control cells. However, the maspin-expressing TM40D-Mp cells had a higher release of cytochrome *c* in the cytosolic fraction when cells were undergoing apoptosis (Fig. 11A, lane 2, cytosolic fraction), which was concurrent with the lower levels of cytochrome *c* in the mitochondrial fraction of the TM40D-Mp cells (Fig. 11A, lane 2, mitochondrial fraction).

To investigate further the translocation of maspin under in vivo conditions when cytochrome *c* is released, immunoprecipitation and Western blotting analysis of whole-cell lysate and mitochondrial and cytosolic fractions for maspin expression were performed (Fig. 11B). Interestingly, we observed an increased level of maspin in the cytoplasmic fraction under noninduced conditions (Fig. 11B, lane 1) compared to induced conditions (Fig. 11B, lane 2), which was concurrent with the translocation of maspin into the mitochondrial fraction under induced conditions. In addition, the level of maspin expression in TM40D-Mp cells under induced conditions is relatively more than under noninduced conditions (Fig. 11B, whole-cell lysate, lanes 1 and 2). These data indicate that under induced conditions, maspin translocates to the mitochondria with the release of cytochrome *c* from the mitochondria.

Use of RNA interference in suppressing the expression of maspin in TM40D-Mp cells. In order to gain further support for the finding that maspin is directly responsible for the increase in apoptosis, we employed RNA interference to specifically downregulate maspin expression in TM40D-Mp cells. Two target sequences starting from nucleotides 229 and 455 of maspin mRNA was designed, and these short interfering RNAs were constructed in the pSUPER.retro vector and transfected into cells in order to obtain cells stably expressing short interfering maspin RNAs. Transfection with short interfering RNA molecules against maspin (si-maspin) effectively suppresses maspin expression in the TM40D-Mp cells (Fig. 12) but not in the control short interfering RNA (containing empty

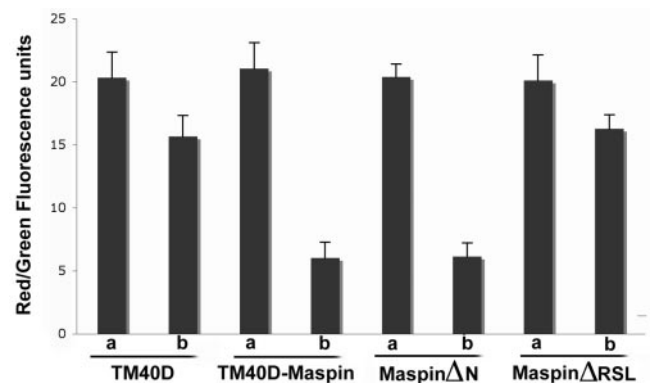


FIG. 10. Loss of $\Delta\Psi_m$. Quantitation was done in both TM40D and TM40D-Mp cells and also in the maspin Δ N and maspin Δ RSL transfectant cells under noninduced (lanes a) and induced conditions (lanes b). As the mitochondrial $\Delta\Psi_m$ collapses (indicating apoptosis), the amount of red fluorescence drops 70 to 75% in TM40D-Mp and maspin Δ N cells and by less than 10% for the TM40D and maspin Δ RSL cells. The bar is a representation from three experimental results of the red/green fluorescence drop.

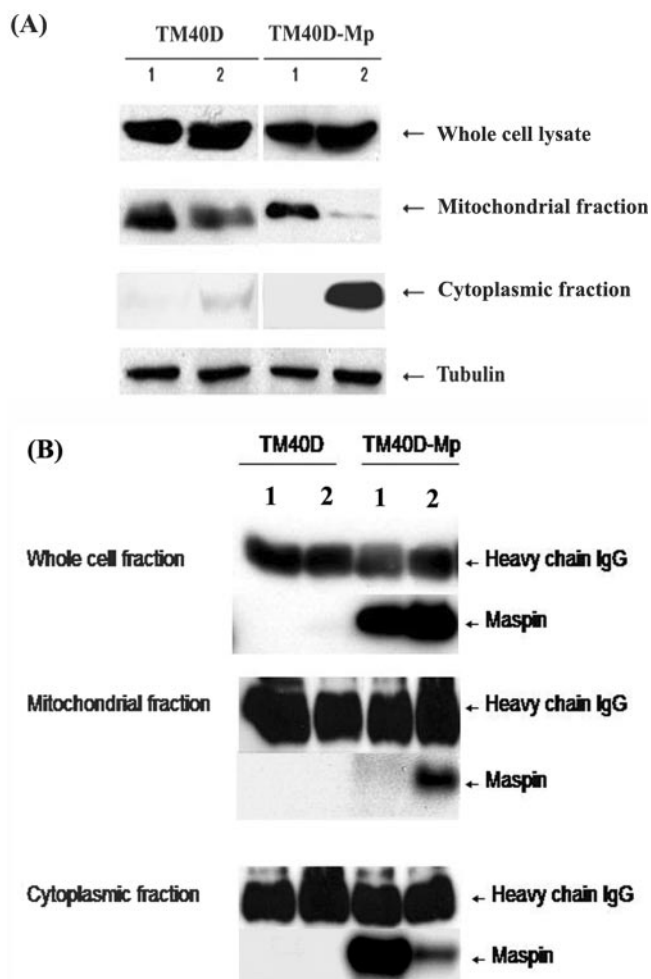


FIG. 11. Release of cytochrome *c* and translocation of maspin *in vivo*. (A) Release of cytochrome *c* from TM40D and TM40D-Mp cells under noninduced (lanes 1) and induced (by 48 h of serum starvation) conditions (lanes 2). The cells were harvested and fractionated, and about 100 μ g of whole-cell lysate/fractionated protein was loaded in an SDS-12.5% PAGE gel and analyzed by Western blotting. Tubulin was used for a loading control. (B) Translocation of maspin to mitochondria in TM40D-Mp cells under noninduced (lane 1) and induced (by 48 h of serum starvation) conditions (lane 2). The cells were harvested and fractionated, and about 2 mg of protein was used for performing the immunoprecipitation analysis with antimaspin and finally analyzed for maspin expression by Western blotting.

vector alone). This was confirmed by immunoprecipitation-Western blotting analysis. As shown in Fig. 12B, the expression of maspin was significantly suppressed in the si-maspin cells (lanes labeled 229 and 445) but not in the cells containing the control short interfering RNA (empty vector alone). The reduction in maspin protein expression was more than 90% complete, as quantified by Western blotting (Fig. 12). However, when the blots were exposed for longer times, there was a faint appearance of maspin expression in the short interfering RNA cells (data not shown).

The caspase 3 activity level measured by the fluorogenic assay is a quantitative analysis for apoptosis in these cells, since downregulated caspase 3 is the final step in the cell death cascade. We therefore measured the caspase 3 activity level in

the control and si-maspin cells to determine the rate of apoptosis. Inhibition of maspin expression resulted in a twofold decrease in the caspase 3 levels of these si-maspin cells (Fig. 12A). We found that the expression of caspase 3 in short interfering RNA-transfected TM40D-Mp cells was reduced by 70% relative to the control-transfected cells or with the control untransfected TM40D-Mp cells. It was interesting that the caspase 3 activity level of these si-maspin cells was similar to that of TM40D cells, which have very low maspin expression. Together, these data demonstrate that maspin is actively involved in the increased induction of apoptosis in TM40D-Mp cells.

DISCUSSION

The purpose of the current study was to investigate the role of maspin in mammary tumor cell apoptosis. In the past few years, maspin has been shown to act as a tumor suppressor, inhibiting both primary tumor growth and metastasis in cell culture. We now report the mediating role of maspin in increasing tumor cell apoptosis. Tumor cells growing *in vivo* have limited access to growth factors, but under normal cell culture conditions, cultured tumor cells grow in the presence of excess serum and growth factors and therefore are less likely to undergo apoptosis. This explains why even in the presence of 10% serum, maspin-expressing cells rarely undergo apoptosis when grown in monolayer cultures (data not shown), as also reported by Jiang et al. (21). Thus, the role of maspin in apoptosis was examined in spheroid tumor cultures.

The three-dimensional model has a distinct advantage for both tumor-tissue interactions and interactions between normal epithelial cells and their surrounding extracellular matrix in making life-and-death decisions (20). In the three-dimensional spheroid model, tumor cells in the center of spheroids have limited growth factors, which more closely mimic solid tumors *in vivo*. Our data demonstrate that the tumor spheroids formed from maspin-expressing tumors had a higher apoptosis rate than those formed from the TM40D control. This finding was confirmed by apoptosis analysis *in vivo* with tumor tissues isolated from implanted tumors. Other *in vitro* experiments showed that the increased apoptosis was autonomously mediated by intracellular maspin. These results are consistent with our previous reports that maspin functioned to induce apoptosis during normal mammary gland development (64).

Maspin belongs to the serine protease inhibitor family of proteins (2), which are well known for their roles in apoptosis. In most cases, serpins function to protect against cell lysis by acting on the cell surface (7, 32) or by inhibiting intracellular proteases such as granzyme B and caspases (4, 55). However, maspin is unique in that it is a noninhibitory serpin that does not inhibit any proteases and can induce cellular apoptosis through mitochondrial translocation. These unique features indicate that the mechanism for maspin-mediated apoptosis is quite different from that found for other serpins. To date, the molecular targets for serpin-mediated apoptosis are not well understood.

Earlier studies by Pemberton et al. (37) revealed that maspin is predominantly a soluble cytoplasmic protein, although small amounts were also found associated with the heavy, light, and nuclear membrane fractions of human mammary epithelial

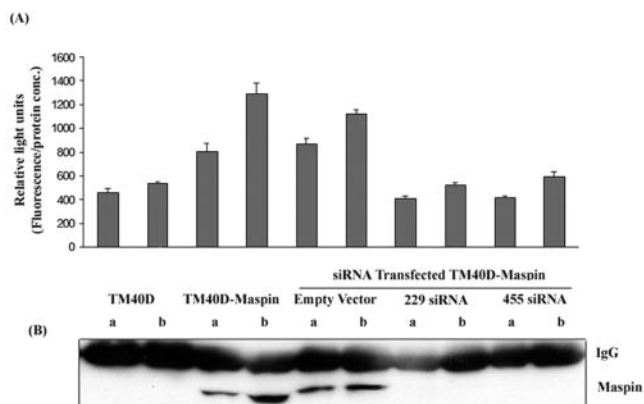


FIG. 12. Suppression of maspin expression in TM40D-Mp cells by RNA interference. (A) Caspase 3 fluorogenic assay of the control (TM40D and TM40D-Mp) cells and short interfering RNA-transfected cells under noninduced (lanes a) and induced (48 h of serum starvation) conditions (lanes b). (B) Maspin protein expression analysis by immunoprecipitation and Western blotting under noninduced (lanes a) and induced (48 h of serum starvation) (lanes b) conditions.

cells. Maass et al. (30) showed that while no maspin expression was detected in cytoplasmic and nuclear lysates obtained from the breast cancer cell line MCF-7, an intense nuclear signal was detected in the pancreatic cancer cell line AsPC-1. Furthermore, Sood et al. (48) reported that the subcellular fractions of two maspin-positive ovarian cancer cell lines contained maspin in both the nuclear and cytoplasmic compartments and also that small amounts of maspin appeared to be associated with distinct structures at the cell surface. In the mouse mammary cell line TM40D-Mp, maspin was expressed in both the cytoplasmic and nuclear fractions as well as in the Golgi bodies and the endoplasmic reticulum. However, a novel finding is that during tumor apoptosis, maspin is translocated to the mitochondria under induced conditions. Therefore, this study focused on the translocation of maspin to mitochondria and the mechanism of maspin-mediated apoptosis.

Mitochondria play a critical role in apoptosis in response to many stimuli. They release proteins into the cytosol, including cytochrome *c*, caspases, AIF, and Smac/DIABLO, in response to a change in permeability of the outer mitochondrial membrane. As a result, mitochondrial proteins are essential for the induction of nuclear apoptosis in vitro in most, if not all, experimental systems of mammalian cell death (29, 52). Moreover, it appears that mitochondria are the principal site of action of Bcl-2 such as oncoproteins. Hence, the study of the regulation of mitochondrial function in vitro, with isolated mitochondria, has an increasing impact on apoptosis research. Here we report for the first time that maspin gets translocated during the import reaction into the mitochondria when the permeability transition pore is induced with atractyloside. Treatment of mitochondria with permeability transition inducers causes the matrix to swell and ultimately ruptures the mitochondrial outer membrane (62). It has been suggested that this effect occurs during apoptosis to cause the loss of $\Delta\Psi_m$ and the release of intermembrane proteins from mitochondria (3). The use of another serpin, ovalbumin, as a control for the import assay proved the specificity of maspin import.

By lowering the sucrose concentration within a mitochondrial suspension, the mitochondrial matrix will swell, leading to rupture of the outer membrane while leaving the inner membrane intact (38). Hence, after swelling of the matrix, proteins that are within or facing the intermembrane space are accessible to externally added protease, resulting in their complete or partial degradation. Galmiche et al. (15) reported that the N-terminal 34-kDa fragment of *Helicobacter pylori* targets mitochondria, and by use of the swelling experiment, p34 and VacA were localized to the inner membrane of the mitochondria. Concurrent with these results, maspin was protected from proteinase K digestion and was present either free in the mitochondrial matrix or associated with the inner membrane after matrix swelling. The carbonate extraction assay was done to further narrow down the localization of imported maspin. This assay involves the extraction of soluble and peripheral membrane proteins from integral membrane proteins through the use of carbonate extraction (13). These data suggests that maspin is translocated to the inner membrane of the mitochondria.

Interestingly, GST-maspin and the mutant with a deletion in the N terminus of maspin were imported whereas, the mutants containing the N terminus alone or the deleted RSL domain did not get imported into the mitochondria. The N-terminal maspin mutant (amino acid 1 to 139) has a large deletion of maspin from amino acids 140 to 375. The inability of N-maspin to import into mitochondria may due to the fact that the deletion of amino acids 140 to 375 removes the functional domain responsible for mitochondrial importing. Deletion of maspin in the N-terminal region confirms that the functional domain is not located in the N terminus of maspin. The maspin Δ N mutant, which loses nearly one-third of maspin (amino acids 1 to 139), is able to import to mitochondria and mediates increased apoptosis (Fig. 8 and 9). This confirms that the functional domain responsible for mitochondrial import is not located in the N-terminal region of maspin. However, a deletion of 35 amino acids in the C-terminal region of maspin, which contains the RSL domain, completely abolishes the ability of maspin to import to mitochondria and to mediate increased apoptosis.

The RSL domain is one of the major functional domains among serpins. Various reports illustrate the importance of the RSL domain of maspin in cell migration and invasion (45) as well as cell-extracellular matrix adhesion (33). However, at least in endothelial cells, deletion of the RSL domain does not affect the function of maspin in antiangiogenesis (65). Here, our result indicates that the RSL domain is also necessary for the translocation of maspin into the mitochondria. Neither the N-maspin nor the maspin Δ RSL transfectant clone induced tumor cell apoptosis. This suggests that the effect of maspin on induced apoptosis may be dictated by unique elements in the RSL sequence.

It is noted that the localization of mutant maspin in the mitochondrial fraction (under induced conditions) in the maspin Δ N transfectant clones is similar to that of intact maspin in TM40D-Mp cells, suggesting that the translocation of maspin (mutant and intact) to the mitochondria might be a crucial step for its role in mediating apoptosis. Considering the increase in the caspase 3 activity level in both TM40D-Mp cells and maspin Δ N cells under induced conditions compared to

induced TM40D cells, we speculate that this increase in the caspase-3 level was the result of increased mitochondrial apoptotic activity in these cells.

Based on these premises, we hypothesize that the permeability transition might be the critical event in determining the apoptosis-inducing potential of maspin. Thus, bringing into focus the question of what supports the import of maspin under the induced permeability transition opening. Pastorino et al. (26) reported the activation of permeability transition by Bax. Depending on the concentration of Bax, a sustained opening of the permeability transition occurred to allow persistent mitochondrial swelling and de-energization. Since the overexpression of Bax also enhances apoptosis through the mitochondrial permeability transition (26), Bax is now known to mediate the apoptosis-sensitizing effect of maspin (28). It has been observed that there is an upregulation of Bax in maspin-expressing cells, but it is largely unknown how Bax regulates the permeability transition at the molecular level. The influence of Bax expression in maspin import to the mitochondria has become the focal point of further study.

Mitochondrial membrane depolarization and cytochrome *c* release from the intermembrane space are supposed to be the determining factors in the final step to apoptosis (29). Recent findings suggest that mitochondrial permeability transition may be an important event in the effector phase of the apoptotic process, wherein the release of cytochrome *c* acts as an essential cofactor in the activation of the dormant killer proteases. Hence, the loss of $\Delta\Psi_m$ under induced conditions both in vitro and in vivo suggests that there is a definite role of permeability transition induction in the import of maspin.

Interestingly, the loss of $\Delta\Psi_m$ was higher in the maspin Δ N transfectant clones than in the maspin Δ RSL clone. Although we cannot exclude the possibility that serum starvation by itself can trigger the mitochondrial pathways of apoptosis, it is important to note that the increased loss of $\Delta\Psi_m$ in the TM40D-Mp cells and the maspin Δ N clones in comparison to the TM40D cells suggests that maspin mediates apoptosis upon induction of the mitochondrial permeability transition. Additionally, the release of cytochrome *c* from the mitochondria into the cytosol correlated with the translocation of maspin into the mitochondria, emphasizing the involvement of an internal signal in this transport machinery. Since maspin is not imported directly, we suspect that maspin might be interacting with another protein which brings maspin to the mitochondria. The involvement of Bcl2 family proteins (such as Bax and Bak) and various other factors that assist maspin translocation to the mitochondria is being investigated. Cross talk from the endoplasmic reticulum is also of interest for future analysis, since the maspin level increases in the endoplasmic reticulum in response to serum starvation.

Finally, to confirm that maspin plays a significant role in increasing the level of apoptosis in these tumor cells, RNA interference was employed to suppress maspin expression. Short interfering RNA-mediated suppression of maspin in TM40D-Mp cells resulted in decreased caspase-3 activity, which was comparable to that of the TM40D parental cells. These data indicate that maspin gets imported into the inner membrane of the mitochondria when the membrane potential is dissipated and is followed by the release of cytochrome *c* into the cytosol through the induction of the permeability transi-

tion. More-detailed studies identifying what causes maspin translocation to the mitochondria are under way.

In summary, this is the first report demonstrating a general mechanism of maspin-mediated tumor cell apoptosis, which occurs through the mitochondrial death pathway. These data indicate that intracellular maspin is translocated to mitochondria in response to an internal signal. Such findings offer a new direction for cancer therapy, wherein identifying the molecular mechanisms of maspin-mediated apoptosis will help to design a better approach for maspin-based therapeutic interventions against breast cancer.

ACKNOWLEDGMENTS

We thank H. Palmieri, Universita di Bari, Bari, Italy, for the OGC antibody. We also thank Xiaodong Wang at UT Southwestern Dallas for helpful discussions. We also thank Jeremy Schaefer for proofreading the manuscript.

This work is supported by DAMD170210294 and NIH grant CA79736 to M.Z.

REFERENCES

1. Addya, S., H. K. Anandatheerthavarada, G. Biswas, A. V. Bhagwat, J. Mullick, and N. G. Avadhani. 1997. Targeting of NH₂-terminal-processed microsomal protein to mitochondria: a novel pathway for the biogenesis of hepatic mitochondrial P450MT2. *J. Cell Biol.* **139**:589–599.
2. Bass, R., A. M. Fernandez, and V. Ellis. 2002. Maspin inhibits cell migration in the absence of protease inhibitory activity. *J. Biol. Chem.* **277**:46845–46848.
3. Bernardi, P., R. Colonna, P. Costantini, O. Eriksson, E. Fontaine, F. Ichas, S. Massari, A. Nicoli, V. Petronilli, and L. Scorrano. 1998. The mitochondrial permeability transition. *Biofactors* **8**:273–281.
4. Bird, C. H., V. R. Sutton, J. Sun, C. E. Hirst, A. Novak, S. Kumar, J. A. Trapani, and P. I. Bird. 1998. Selective regulation of apoptosis: the cytotoxic lymphocyte serpin proteinase inhibitor 9 protects against granzyme B-mediated apoptosis without perturbing the Fas cell death pathway. *Mol. Cell Biol.* **18**:6387–6398.
5. Budihardjo, I., H. Oliver, M. Lutter, X. Luo, and X. Wang. 1999. Biochemical pathways of caspase activation during apoptosis. *Annu. Rev. Cell Dev. Biol.* **15**:269–290.
6. Chinnaiyan, A. M., K. O'Rourke, M. Tewari, and V. M. Dixit. 1995. FADD, a novel death domain-containing protein, interacts with the death domain of Fas and initiates apoptosis. *Cell* **81**:505–512.
7. Dickinson, J. L., B. J. Norris, P. H. Jensen, and T. M. Antalis. 1998. The C-2 interhelical domain of the serpin plasminogen activator inhibitor-type 2 is required for protection from TNF-alpha induced apoptosis. *Cell Death Differ.* **5**:163–171.
8. Du, C., M. Fang, Y. Li, L. Li, and X. Wang. 2000. Smac, a mitochondrial protein that promotes cytochrome c-dependent caspase activation by eliminating IAP inhibition. *Cell* **102**:33–42.
9. Elbashir, S. M., J. Harborth, K. Weber, and T. Tuschl. 2002. Analysis of gene function in somatic mammalian cells using small interfering RNAs. *Methods* **26**:199–213.
10. Evan, G. I., and K. H. Vousden. 2001. Proliferation, cell cycle and apoptosis in cancer. *Nature* **411**:342–348.
11. Finkel, E. 1999. Does cancer therapy trigger cell suicide? *Science* **286**:2256–2258.
12. Finucane, D. M., E. Bossy-Wetzel, N. J. Waterhouse, T. G. Cotter, and D. R. Green. 1999. Bax-induced caspase activation and apoptosis via cytochrome c release from mitochondria is inhibitable by Bcl-xL. *J. Biol. Chem.* **274**:2225–2233.
13. Fujiki, Y., S. Fowler, H. Shio, A. L. Hubbard, and P. B. Lazarow. 1982. Polypeptide and phospholipid composition of the membrane of rat liver peroxisomes: comparison with endoplasmic reticulum and mitochondrial membranes. *J. Cell Biol.* **93**:103–110.
14. Futscher, B. W., M. M. Oshiro, R. J. Wozniak, N. Holtan, C. L. Hanigan, H. Duan, and F. E. Domann. 2002. Role for DNA methylation in the control of cell type specific maspin expression. *Nat. Genet.* **31**:175–179.
15. Galmiche, A., J. Rassow, A. Doye, S. Cagnol, J. C. Chambard, S. Contamin, T. de V., I. Just, V. Ricci, E. Solcia, E. Van Obberghen, and P. Boquet. 2000. The N-terminal 34 kDa fragment of Helicobacter pylori vacuolating cytotoxin targets mitochondria and induces cytochrome c release. *EMBO J.* **19**:6361–6370.
16. Hacki, J., L. Egger, L. Monney, S. Conus, T. Rosse, I. Fellay, and C. Borner. 2000. Apoptotic crosstalk between the endoplasmic reticulum and mitochondria controlled by Bcl2. *Oncogene* **19**:2286–2295.

17. Hanahan, D., and R. A. Weinberg. 2000. The hallmarks of cancer. *Cell* **100**:57–70.
18. Hobbs, S., S. Jitrapakdee, and J. C. Wallace. 1998. Development of a Bicistronic Vector driven by the Human polypeptide chain elongation factor 1 α promoter for creation of stable mammalian cell lines that express very high levels of recombinant proteins. *Biochem. Biophys. Res. Commun.* **252**:368–372.
19. Hu, Y., M. A. Benedict, L. Ding, and G. Nunez. 1999. Role of cytochrome c and dATP/ATP hydrolysis in Apaf-1-mediated caspase-9 activation and apoptosis. *EMBO J.* **18**:3586–3595.
20. Jacks, T., and R. A. Weinberg. 2002. Taking the study of cancer cell survival to a new dimension. *Cell* **111**:923–925.
21. Jiang, N., Y. Meng, S. Zhang, E. Mensah-Osman, and S. Sheng. 2002. Maspin sensitizes breast carcinoma cells to induced apoptosis. *Oncogene* **21**:4089–4098.
22. Kittrell, F. S., C. J. Oborn, and D. Medina. 1992. Development of mammary preneoplasias in vivo from mouse mammary epithelial cell lines in vitro. *Cancer Res.* **52**:1924–1932.
23. Kluck, R. M., E. Bossy-Wetzel, D. R. Green, and D. D. Newmeyer. 1997. The release of cytochrome c from mitochondria: a primary site for Bcl-2 regulation of apoptosis. *Science* **275**:1132–1136.
24. Kroemer, G., P. Petit, N. Zamzami, J. L. Vayssiere, and B. Mignotte. 1995. The biochemistry of programmed cell death. *FASEB J.* **9**:1277–1287.
25. Li, H., H. Zhu, C. J. Xu, and J. Yuan. 1998. Cleavage of BID by caspase 8 mediates the mitochondrial damage in the Fas pathway of apoptosis. *Cell* **94**:491–501.
26. Li, J. J., N. H. Colburn, and L. W. Oberley. 1998. Maspin gene expression in tumor suppression induced by overexpressing manganese-containing superoxide dismutase cDNA in human breast cancer cells. *Carcinogenesis* **19**:833–839.
27. Li, L. Y., X. Luo, and X. Wang. 2001. Endonuclease G is an apoptotic DNase when released from mitochondria. *Nature* **412**:95–99.
28. Liu, J., S. Yin, N. Reddy, C. Spencer, and S. Sheng. 2004. Bax mediates the apoptosis-sensitizing effect of maspin. *Cancer Res.* **64**:1704–1711.
29. Liu, X., H. Zou, C. Slaughter, and X. Wang. 1997. DFF, a heterodimeric protein that functions downstream of caspase-3 to trigger DNA fragmentation during apoptosis. *Cell* **89**:175–184.
30. Maass, N., L. Rolver, M. Ziebart, K. Nagasaki, and P. Rudolph. 2002. Maspin locates to the nucleus in certain cell types. *J. Pathol.* **197**:272–274.
31. Marx, J. 2002. Cancer research. Obstacle for promising cancer therapy. *Science* **295**:1444.
32. McGettrick, A. F., R. C. Barnes, and D. M. Worrall. 2001. SCCA2 inhibits TNF-mediated apoptosis in transfected HeLa cells. The reactive centre loop sequence is essential for this function and TNF-induced cathepsin G is a candidate target. *Eur. J. Biochem.* **268**:5868–5875.
33. Ngamkitidechakul, C., D. J. Warejcka, J. M. Burke, W. J. O'Brien, and S. S. Twining. 2003. Sufficiency of the reactive site loop of maspin for induction of cell-matrix adhesion and inhibition of cell invasion. Conversion of ovalbumin to a maspin-like molecule. *J. Biol. Chem.* **278**:31796–31806.
34. Nguyen, M., D. G. Millar, V. W. Yong, S. J. Korsmeyer, and G. C. Shore. 1993. Targeting of Bcl-2 to the mitochondrial outer membrane by a COOH-terminal signal anchor sequence. *J. Biol. Chem.* **268**:25265–25268.
35. Pastorino, J. G., M. Tafani, R. J. Rothman, A. Marcineviute, J. B. Hoek, and J. L. Farber. 1999. Function consequences of the sustained or transient activation by Bax of the mitochondria permeability transition pore. *J. Biol. Chem.* **274**:31734–31739.
36. Pedersen, P. L., J. W. Greenawalt, B. Reynafarje, J. Hullihen, G. L. Decker, J. W. Soper, and E. Bustamante. 1978. Preparation and characterization of mitochondria and submitochondrial particles of rat liver and liver-derived tissues. *Methods Cell Biol.* **20**:411–481.
37. Pemberton, P. A., A. R. Tipton, N. Pavloff, J. Smith, J. R. Ericson, Z. M. Mouchabeck, and M. C. Kiefer. 1997. Maspin is an intracellular serpin that partitions into secretory vesicles and is present at the cell surface. *J. Histochem. Cytochem.* **45**:1697–1706.
38. Petit, P. X., M. Goubern, P. Dirolez, S. A. Susin, N. Zamzami, and G. Kroemer. 1998. Disruption of the outer mitochondrial membrane as a result of large amplitude swelling: the impact of irreversible permeability transition. *FEBS Lett.* **426**:111–116.
39. Ravagnan, L., I. Marzo, P. Costantini, S. A. Susin, N. Zamzami, P. X. Petit, F. Hirsch, M. Goubern, M. F. Poupon, L. Miccoli, Z. Xie, J. C. Reed, and G. Kroemer. 1999. Lonidamine triggers apoptosis via a direct, Bcl-2-inhibited effect on the mitochondrial permeability transition pore. *Oncogene* **18**:2537–2546.
40. Reers, M., S. T. Smiley, C. Mottola-Hartshorn, A. Chen, M. Lin, and L. B. Chen. 1995. Mitochondrial membrane potential monitored by JC-1 dye. *Methods Enzymol.* **260**:406–417.
41. Ricci, J. E., R. A. Gottlieb, and D. R. Green. 2003. Caspase-mediated loss of mitochondrial function and generation of reactive oxygen species during apoptosis. *J. Cell Biol.* **160**:65–75.
42. Ryan, M. T., W. Voos, and N. Pfanner. 2001. Assaying protein import into mitochondria. *Methods Cell Biol.* **65**:189–215.
43. Sager, R., S. Sheng, P. Pemberton, and M. J. Hendrix. 1996. Maspin: a tumor suppressing serpin. *Curr. Top. Microbiol. Immunol.* **213**:51–64.
44. Santini, M. T., and G. Rainaldi. 1999. Three-dimensional spheroid model in tumor biology. *Pathobiology* **67**:148–157.
45. Sheng, S., J. Carey, E. A. Seftor, L. Dias, M. J. Hendrix, and R. Sager. 1996. Maspin acts at the cell membrane to inhibit invasion and motility of mammary and prostatic cancer cells. *Proc. Natl. Acad. Sci. USA* **93**:11669–11674.
46. Shi, H. Y., W. Zhang, R. Liang, S. Abraham, F. S. Kittrell, D. Medina, and M. Zhang. 2001. Blocking tumor growth, invasion, and metastasis by maspin in a syngeneic breast cancer model. *Cancer Res.* **61**:6945–6951.
47. Sollner, T., J. Rassow, and N. Pfanner. 1991. Analysis of mitochondrial protein import using translocation intermediates and specific antibodies. *Methods Cell Biol.* **34**:345–358.
48. Sood, A. K., M. S. Fletcher, L. M. Gruman, J. E. Coffin, S. Jabbari, Z. K. Ellis, N. Arbour, E. A. Seftor, and M. J. C. Hendrix. 2002. The Paradoxical expression of maspin in ovarian carcinoma. *Clin. Cancer Res.* **8**:2924–2932.
49. Sternlicht, M. D., P. Kedeshian, Z. M. Shao, S. Safarians, and S. H. Barsky. 1997. The human myoepithelial cell is a natural tumor suppressor. *Clin. Cancer Res.* **3**:1949–1958.
50. Stolzenberg, I., S. Wulf, H. G. Mannherz, and R. Paddenberg. 2000. Different sublines of Jurkat cells respond with varying susceptibility of internucleosomal DNA degradation to different mediators of apoptosis. *Cell Tissue Res.* **301**:273–282.
51. Susin, S. A., N. Zamzami, M. Castedo, T. Hirsch, P. Marchetti, A. Macho, E. Daugas, M. Geuskens, and G. Kroemer. 1996. Bcl-2 inhibits the mitochondrial release of an apoptogenic protease. *J. Exp. Med.* **184**:1331–1341.
52. Susin, S. A., H. K. Lorenzo, N. Zamzami, I. Marzo, B. E. Snow, G. M. Brothers, J. Mangion, E. Jacotot, P. Costantini, M. Loeffler, N. Larochette, D. R. Goodlett, R. Aebersold, D. P. Siderovski, J. M. Penninger, and G. Kroemer. 1999. Molecular characterization of mitochondrial apoptosis-inducing factor. *Nature* **397**:441–446.
53. Sutherland, R. M., J. A. McCredie, and W. R. Inch. 1971. Growth of multicell spheroids in tissue culture as a model of nodular carcinomas. *J. Natl. Cancer Inst.* **46**:113–120.
54. Suzuki, Y., Y. Imai, H. Nakayama, K. Takahashi, K. Takio, and R. Takahashi. 2001. A serine protease, HtrA2, is released from the mitochondria and interacts with XIAP, inducing cell death. *Mol. Cell* **8**:613–621.
55. Tewari, M., W. G. Telford, R. A. Miller, and V. M. Dixit. 1995. CrmA, a poxvirus-encoded serpin, inhibits cytotoxic T-lymphocyte-mediated apoptosis. *J. Biol. Chem.* **270**:22705–22708.
56. Verhagen, A. M., P. G. Ekert, M. Pakusch, J. Silke, L. M. Connolly, G. E. Reid, R. L. Moritz, R. J. Simpson, and D. L. Vaux. 2000. Identification of DIABLO, a mammalian protein that promotes apoptosis by binding to and antagonizing IAP proteins. *Cell* **102**:43–53.
57. Voisine, C., E. A. Craig, N. Zufall, O. von Ahlsen, N. Pfanner, and W. Voos. 1999. The protein import motor of mitochondria: unfolding and trapping of preproteins are distinct and separable functions of matrix Hsp70. *Cell* **97**:565–574.
58. Wang, M. C., Y. M. Yang, X. H. Li, F. Dong, and Y. Li. 2004. Maspin expression and its clinicopathological significance in tumorigenesis and progression of gastric cancer. *World J. Gastroenterol.* **10**:634–637.
59. Waterhouse, N. J., J. C. Goldstein, R. M. Kluck, D. D. Newmeyer, and D. R. Green. 2001. The (Holey) study of mitochondria in apoptosis. *Methods Cell Biol.* **66**:365–391.
60. Yang, J., X. Liu, K. Bhalla, C. N. Kim, A. M. Ibrado, J. Cai, T. I. Peng, D. P. Jones, and X. Wang. 1997. Prevention of apoptosis by Bcl-2: release of cytochrome c from mitochondria blocked. *Science* **275**:1129–1132.
61. Zamzami, N., P. Marchetti, M. Castedo, C. Zanin, J. L. Vayssiere, P. X. Petit, and G. Kroemer. 1995. Reduction in mitochondrial potential constitutes an early irreversible step of programmed lymphocyte death in vivo. *J. Exp. Med.* **181**:1661–1672.
62. Zamzami, N., P. Marchetti, M. Castedo, T. Hirsch, S. A. Susin, B. Masse, and G. Kroemer. 1996. Inhibitors of permeability transition interfere with the disruption of the mitochondrial transmembrane potential during apoptosis. *FEBS Lett.* **384**:53–57.
63. Zhang, M., N. Maass, D. Magit, and R. Sager. 1997. Transactivation through Ets and Ap1 transcription sites determines the expression of the tumor-suppressing gene maspin. *Cell Growth Differ.* **8**:179–186.
64. Zhang, M., D. Magit, F. Botteri, H. Y. Shi, K. He, M. Li, P. Furth, and R. Sager. 1999. Maspin plays an important role in mammary gland development. *Dev. Biol.* **215**:278–287.
65. Zhang, M., Y. Shi, D. Magit, P. A. Furth, and R. Sager. 2000. Maspin is an angiogenesis inhibitor. *Nat. Med.* **6**:196–199.
66. Zou, H., Y. Li, X. Liu, and X. Wang. 1999. An APAF-1/cytochrome c multimeric complex is a functional apoptosome that activates procaspase-9. *J. Biol. Chem.* **274**:11549–11556.
67. Zou, Z., A. Anisowicz, M. J. Hendrix, A. Thor, M. Neveu, S. Sheng, K. Rafidi, E. Seftor, and R. Sager. 1994. Maspin, a serpin with tumor-suppressing activity in human mammary epithelial cells. *Science* **263**:526–529.
68. Zou, Z., C. Gao, A. K. Nagaich, T. Connell, S. Saito, J. W. Moul, P. Seth, E. Appella, and S. Srivastava. 2000. p53 regulates the expression of the tumor suppressor gene maspin. *J. Biol. Chem.* **275**:6051–6054.